Diversity and Distributions, (Diversity Distrib.) (2017) **23**, 421–434

BIODIVERSITY RESEARCH

Climate variability drives population cycling and synchrony

Lars Y. Pomara* and Benjamin Zuckerberg

Department of Forest and Wildlife Ecology, University of Wisconsin-Madison, Madison, WI 53706, USA

ABSTRACT

Aim There is mounting concern that climate change will lead to the collapse of cyclic population dynamics, yet the influence of climate variability on population cycling remains poorly understood. We hypothesized that variability in survival and fecundity, driven by climate variability at different points in the life cycle, scales up from local populations to drive regional characteristics of population cycling and spatial synchronization.

Location Forest in the US Upper Midwest and Great Lakes region.

Methods We tested hypotheses linking variation in vital rates of Ruffed Grouse (*Bonasa umbellus*), a declining species that displays decadal population cycles, to temperature and precipitation anomalies and land use intensity, using rate estimates from multiple locations in eastern North America. We used climate-demographic linkages to simulate spatially explicit population dynamics from 1982 to 2069, evaluated predictions against monitoring data and assessed predicted population dynamics under future climate projections.

Results Nest success and winter survival were linked to temperature and precipitation anomalies, and demographic models explained important spatio-temporal characteristics of cycling and synchrony in monitoring data. The climate-driven vital rates were necessary for cycling and synchrony in models, even though the four included climate variables were not individually periodic. Cycling and synchrony were stronger at more northerly latitudes, but this transition occurred abruptly, reflecting regional variation in winter conditions. Forecasts suggested climate-driven cycling through mid-century, followed by desynchronization and dampening.

Main conclusions Climate variability can drive spatio-temporal variation in demographic rates, and population cycling can result from these relationships. Pathways linking climate to broad-scale population dynamics involve responses of vital rates to several climate variables at different times of year and may be more complex than direct responses to known modes of climate variability. The wide-ranging impact of climate change on the demographics of northerly adapted species has the potential to degrade patterns of population synchrony and cycling.

*Correspondence: Lars Y. Pomara, Southern Research Station, USDA Forest Service, 200 WT Weaver Blvd, Asheville, NC 28804, USA. E-mail: lazarusypomara@fs.fed.us

Keywords

climate change vulnerability, climate-driven vital rates, population cycling, Ruffed Grouse, spatial synchrony, spatially explicit demographic model.

INTRODUCTION

Several biotic and abiotic mechanisms have been offered to explain the cyclic population dynamics exhibited by many terrestrial species in high-latitude ecosystems. Predator–prey interactions and delayed density dependence have traditionally played key roles in models, but recently, the role of climate variability has received increasing attention and support (Krebs *et al.*, 2001; Aars & Ims, 2002; Krebs, 2011; Hansen *et al.*, 2013). Cyclic population dynamics have been reconstructed using models that combine influences of climate and density dependence for several taxa including

DOI: 10.1111/ddi.12540
http://wileyonlinelibrary.com/journal/ddi

Snowshoe Hare (*Lepus americanus*) in North America and rodents in Norway (Kausrud *et al.*, 2008; Yan *et al.*, 2013). Given that high-latitude ecosystems have been disproportionately exposed to rapid warming in recent decades, understanding the influence of climate variability on cyclic dynamics and their demographic mechanisms will be increasingly important for assessing impacts of future climate change on northerly species (Ims *et al.*, 2008; Post *et al.*, 2009; Hansen *et al.*, 2013; Hartmann *et al.*, 2013).

There is mounting evidence that long-term population fluctuations of winter-adapted species are influenced by changes in weather and climate variability. In high-latitude environments, biotic interactions and population dynamics are often mediated by the indirect and direct effects of winter weather (Hansson & Henttonen, 1985; Ranta *et al.*, 1995; Williams *et al.*, 2004). Winter-adapted species must cope with variability in seasonality and changes in the depth, quality and persistence of snow cover (Lindström & Hörnfeldt, 1994; Aars & Ims, 2002; Tyler *et al.*, 2008). For example, long-term fluctuations of Fennoscandian rodent populations were influenced by interannual winter temperature variability which impacted snow cover and the quality of subnivean space (Kausrud *et al.*, 2008). In the high Arctic, extreme winter weather such as heavy rain-on-snow events mediated biotic interactions between herbivores and their predators and synchronized population fluctuations for multiple species (Hansen *et al.*, 2013). Cornulier *et al.* (2013) found that altered and dampening cycles in vole populations across Europe were likely a result of large-scale environmental variability that influenced winter population growth rates, as opposed to direct or delayed density dependence.

An important line of evidence linking climate to population cycling has been the regional nature of cyclic dynamics. Local dynamics of cycling species tend to be synchronized across broad regions, and in many taxa, cycling dampens at lower latitudes – a phenomenon thought to be associated with climatology (particularly shortening winters) and broad-scale changes in land cover (Hansson & Henttonen, 1985; Ranta *et al.*, 1995; Williams *et al.*, 2004; Ims *et al.*, 2008). Modern climate change and rising ambient temperatures may be accompanied by increasingly synchronized patterns of climate variability, which can strengthen synchronization of population dynamics at regional scales (Post & Forchhammer, 2004; Koenig & Liebhold, 2016).

Quantifying the influence of climate variability on population cycling has relied on analysing time series of abundance collected by monitoring programmes, but there is a need to understand the demographic mechanisms underlying these population changes (Jenouvrier, 2013; Selwood *et al.*, 2014). Identifying sensitivities to climate variability at critical demographic stages in a species' life cycle is essential for uncovering climate-demography mechanisms associated with cycling. Ruffed Grouse (*Bonasa umbellus*) is an exemplary winter-adapted Galliform species inhabiting northern forests of North America (Rusch *et al.*, 2000). Ruffed Grouse exhibits decadal population cycles, but cycle amplitude diminishes southward, and the most southerly populations do not cycle (Keith & Rusch, 1989; Williams *et al.*, 2004; Tirpak *et al.*, 2006). Winter is a crucial time and demographic bottleneck for Ruffed Grouse, as they have low fat and protein reserves and little metabolic resistance to fasting. During winter, predation by mammals and avian predators is a primary source (> 80%) of mortality (Thomas, 1987; Tirpak *et al.*, 2006; Devers *et al.*, 2007). Ruffed Grouse use snow cover as a refuge, burrowing into "snow roosts" for predator avoidance and thermal cover when deep and light snow is present, reducing metabolic heat production by 30% (Thompson & Fritzell, 1988). The influence of winter weather on grouse demographics has received less attention than trophic interactions (e.g. predation), probably because winter weather conditions are not considered limiting for southerly populations. However, in northern Minnesota, where snow cover typically persists through winter, grouse cycling was best explained by an interaction between winter precipitation and minimum temperature – cold winters with high precipitation were correlated with increasing springtime population numbers, presumably due to high winter survival (Zimmerman *et al.*, 2008).

Little is known about relationships between climate and fecundity in Ruffed Grouse, but there is evidence for a negative relationship between summer precipitation and both hatching success and brood survival in many high-latitude, cycling grouse species due to negative thermal effects on eggs and precocial chicks, depressed arthropod food abundance and higher predation rates, under inclement conditions (Hannon & Martin, 2006). Black Grouse (*Tetrao tetrix*) population growth rate in northern Italy correlated negatively with early summer precipitation (Viterbi *et al.*, 2015). Black Grouse in Finland responded to earlier springs by advancing egg-laying and hatching, but because early summer conditions remained unchanged, young were exposed to a colder post-hatching environment and suffered high mortality (Ludwig *et al.*, 2006). This demographic mismatch caused by asynchronous climate change reduced the probability of observing cyclic dynamics.

Our goal was to assess the influence of past and future climate variability on the spatio-temporal characteristics of Ruffed Grouse population cycling and synchrony. We first tested whether winter survival and nest success were influenced by winter and breeding season climate variability, respectively, by linking vital rate estimates from multiple demographic studies to locality- and season-specific climate data. We then developed a spatially explicit demographic model that integrated these climate sensitivities, exposure to spatio-temporal climate variability, land cover characteristics and dispersal (Pulliam *et al.*, 1992; Schurr *et al.*, 2012; Fordham *et al.*, 2013). Spatial coupling of climate variability with population dynamics across a large region allowed us to investigate cycling and spatial synchrony in an integrated framework. Using this model, we tested the hypothesis that variability in survival and fecundity, driven by climate variability at different points in the life cycle, scales up from

local populations to drive regional characteristics of cycling and synchronization. Using climate projections, we then explored the consequences of future climate change (Fischer & Knutti, 2015) for regional population dynamic characteristics and assessed the possibility of dampened cycling.

We focused on Ruffed Grouse populations in the Upper Midwestern United States including Minnesota, Wisconsin and Michigan (Fig. 1). Mean temperature in this region increased at a trend of 0.5 °C decade^{-1} from 1970 to 2005, with concurrent increases in spring, summer and autumn precipitation (Lorenz *et al.*, 2009; Pryor *et al.*, 2009). North American snow cover has declined since the mid-20th century, and climate models suggest future decline throughout the Upper Midwest, with attenuating winters characterized by more rain-on-snow events (Kapnick & Delworth, 2013; Krasting *et al.*, 2013; Notaro *et al.*, 2014). We characterized population fluctuations in grouse monitoring data and in model results in terms of periodicity, magnitude and spatial synchrony across this region.

METHODS

We modelled demographic rates based on an analysis of published data, then constructed a spatially explicit demographic model, evaluated model performance across a historical period with independent monitoring data and finally characterized future model projections.

Vital rate modelling

To quantify the sensitivity (Williams *et al.*, 2008) of demographic rates to environmental variability, we tested hypotheses relating non-breeding survival and nest success estimates to climate and land use, in an information–theoretic framework (Burnham & Anderson, 2002). These two vital rates are crucial to the demography of Ruffed Grouse and have been extensively studied (Rusch *et al.*, 2000; Devers *et al.*, 2007). We included estimates of non-breeding season (September to February) survival rates and nest success rates available from radio telemetry studies within and outside our study region, but all were in the eastern United States (Fig. 1; Table S1 in Supporting Information). This allowed us to base vital rate models on the broadest available sampling of environmental variability. Unavoidably, some climatic conditions within the study region were not represented by the available survival and nest success studies, especially in the most northerly part of the region.

For predictor variables, we relied on spatio-temporal data sets for which comparable future projection data were available, and we matched annual values to the vital rate study locations and years. Annual minimum and maximum temperature (mean temperature of the coldest month and of the warmest month, respectively; °C) and precipitation (of the wettest and of the driest month; mm day^{-1}) anomalies were developed from monthly data from 1950 to 2012 using the

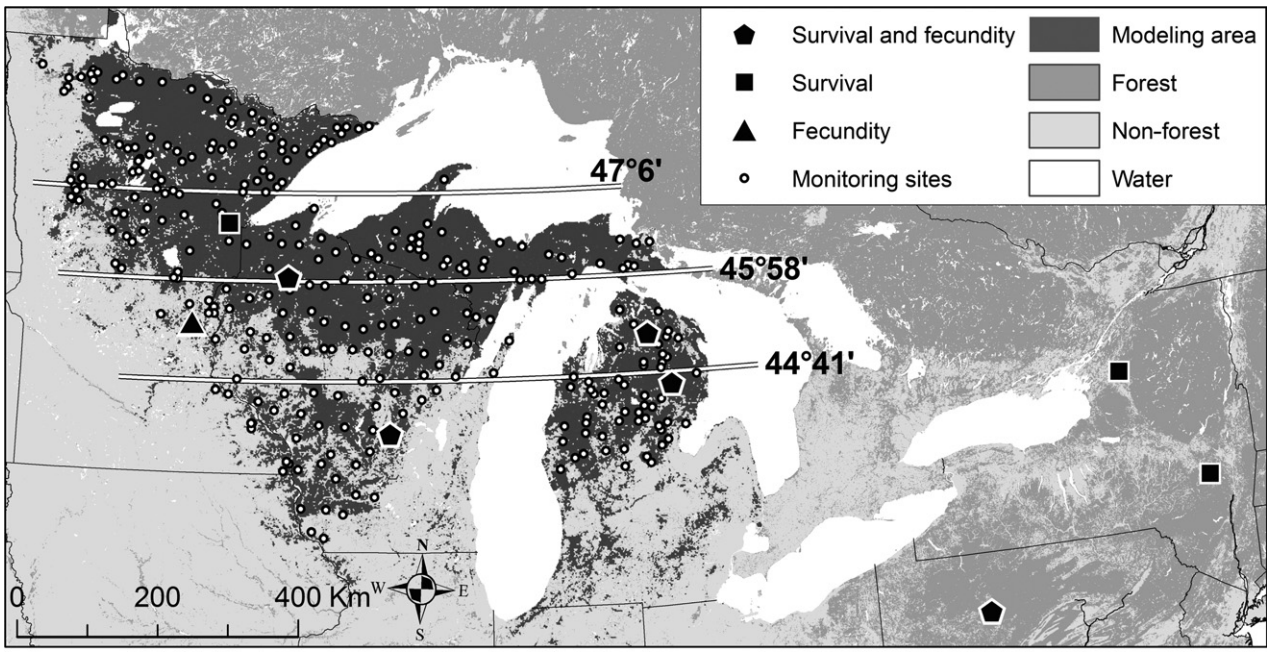

Figure 1 Ruffed Grouse vital rate study sites, demographic modelling region, and monitoring sites. Vital rate study sites were widely dispersed within and outside the demographic modelling region, which included only forest-dominated landscapes within the US states of Minnesota, Wisconsin, and Michigan. Five additional nest success study sites, located further south in the Appalachian Mountains, are not shown. Long-term population monitoring sites within the demographic modelling region were also situated within forest. The latitudinal divisions used to group the monitoring sites for statistical summaries were chosen such that each group contained an equal number of sites (n = 76).

Parameter-elevation Relationships on Independent Slopes Model (PRISM) data (Daly *et al.*, 2008). In the study region, precipitation in the wettest and driest months always occurred in summer and winter months, respectively. For future projection, the same variables were developed for 1950–2069 from the World Climate Research Program's (WCRP) Coupled Model Intercomparison Project phase 5 (CMIP5) multimodel ensemble, downloaded from the Bias Corrected and Downscaled WCRP CMIP5 Climate Projections archive (Taylor *et al.*, 2012). Future projection models were for Representative Concentration Pathway 4.5, a moderate warming trajectory. We also accounted for land use intensification in and near forest, although we did not expect these unidirectional changes (i.e. increasing land use intensity) to contribute to cyclical population dynamics. We used estimates of change in housing density based on the US Decennial Census; these estimates are strongly correlated with landscape fragmentation (Radeloff *et al.*, 2010). We calculated density within a 5-km-radius circle around each study site, to approximate an ecologically relevant landscape context. Additional details for the development of demographic rate, climate and land use data are provided in Appendix S1.

We modelled survival and nest success estimates with three main effects – temperature, precipitation and housing density – including the two winter weather variables for non-breeding survival and the two summer weather variables for nest success. We were particularly interested in how the winter precipitation–temperature interaction might influence non-breeding survival (Fig. 2a). Winter temperature is expected to modulate the quality of snow cover for snow roosting, and likewise, snow cover should modulate the direct effects of temperature variability (Aars & Ims, 2002; Kausrud *et al.*, 2008; Zimmerman *et al.*, 2008). In the absence of interactions, we expected unimodal (peaked) relationships of both vital rates with both temperature and precipitation anomalies. An exception was summer precipitation (Fig. 2b), for which a negative relationship with both nest success and brood survival has been proposed (Hannon & Martin, 2006; Viterbi *et al.*, 2015). We expected that housing

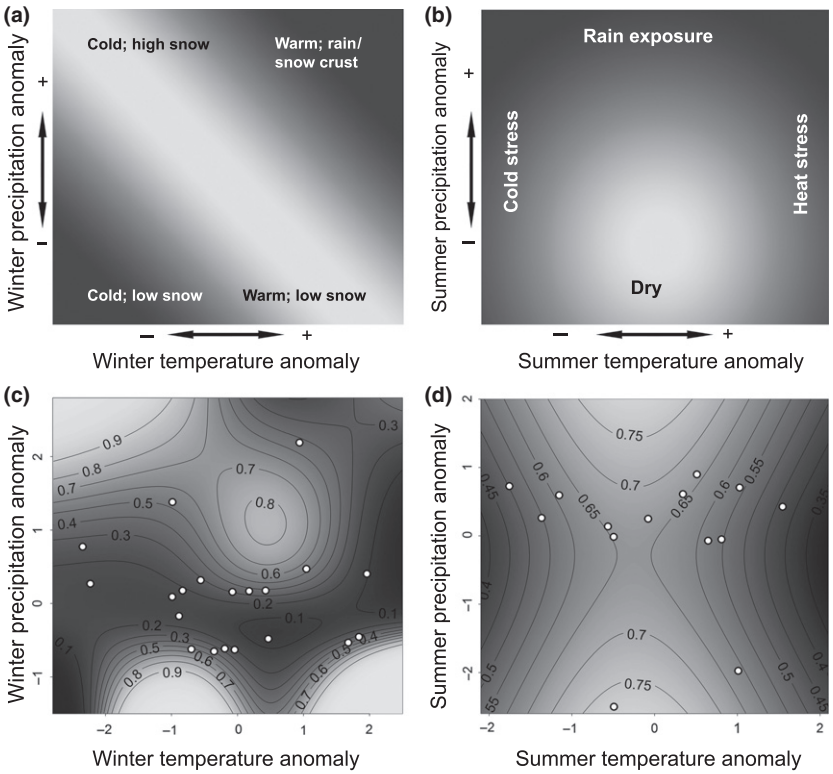

Figure 2 Hypothesized (a, b) and modelled (c, d) effects of winter and breeding season climate conditions on Ruffed Grouse non-breeding survival and nest success, respectively. Lighter shades represent higher expected survival and nest success, and points indicate the vital rate samples used to build the models. Climate anomaly values are standardized. Winter temperature and precipitation anomalies should have an interactive influence on overwintering survival. At high precipitation, low temperatures promote deeper, less compacted snow more suitable for roosting; whereas higher temperatures promote rain or snow crusting and compaction, resulting in a negative relationship between temperature and survival. At low winter precipitation and low snow roost availability, high thermal exposure is expected to result in a positive relationship between temperature and survival. High or low breeding season temperature extremes may suppress nest success, whereas we expected a negative relationship with precipitation. We used the highest-support Generalized Additive Model prediction surfaces shown here (c, d) to project vital rate variability in the demographic model, spatially and over time.

density would capture additional negative effects associated with land use and forest fragmentation. Based on these relationships, we developed four models of interest for each vital rate (Table 1). None of the predictor variables showed high collinearity for either data set ($R < 0.6$; Dormann *et al.*, 2013).

Given their potentially nonlinear relationships with climate variables, we modelled the two vital rates using generalized additive models (GAMs) with binomial error distribution and a logit link function. The GAMs fit smooth functions using penalized regression splines with smoothing parameters selected by minimizing the unbiased risk estimator (UBRE), which scales with Akaike's information criterion (AIC; Wood, 2006). We used cubic regression splines (*s*) for predictor variables in models with additive structure and a tensor product smooth (*te*) to represent the interaction between temperature and precipitation (Wood, 2006). After a smoothing term for housing density did not improve models, it was entered as a linear term. We accounted for the number of trials contributing to the different survival and nest success estimates (i.e. telemetered individuals or monitored nests) by weighting estimates by their sample size (Table S1; Zuur *et al.*, 2009). We used the sample size adjusted AIC (AIC_c) to rank models and assessed variable importance with summed Akaike weights for the full model set (Burnham & Anderson, 2002). Models and model selection were implemented in R, using the MGCV package and base functions (Wood, 2006; R Core Team, 2014).

Table 1 Model selection results for Ruffed Grouse non-breeding season survival and nest success generalized additive models.

	UBRE	AIC_c	ΔAIC_c	w_i
Non-breeding season survival				
te(mintemp, minprecip) + HD	0.936	128.9	0.0	0.875
te(mintemp, minprecip)	1.135	132.8	3.9	0.125
s(mintemp) + *s*(minprecip)	4.891	206.5	77.6	0.000
s(mintemp) + *s*(minprecip) + HD	4.943	207.4	78.5	0.000
Intercept only	6.453	236.9	108.0	0.000
Nest success				
s(maxtemp) + *s*(maxprecip)	0.575	50.79	0.00	0.477
s(maxtemp) + *s*(maxprecip) + HD	0.712	52.15	1.36	0.242
te(maxtemp, maxprecip)	0.780	52.86	2.07	0.169
te(maxtemp, maxprecip) + HD	0.921	54.26	3.47	0.084
Intercept only	1.154	56.51	5.73	0.027

We retained the top model ($\Delta AIC_c = 0$) for each vital rate, for projecting rates in the subsequent demographic simulation. Cubic regression spline smoothing parameters are indicated by *s*(), and tensor product smooths incorporating interaction effects are indicated by *te*(). Mintemp = temperature in the coldest month; minprecip = precipitation in the driest month; maxtemp = temperature in the warmest month; maxprecip = precipitation in the wettest month; HD = housing density within a 5 km radius surrounding the study site. UBRE = unbiased risk estimator; w_i = model weight.

Spatially explicit demographic modelling

We modelled the population-level consequences of climate and land use effects identified in the vital rate models using an individual-based, stochastic simulation framework in the HexSim platform (McRae *et al.*, 2008; Lurgi *et al.*, 2015). Individuals occupied a grid of hexagonal, 2-km-wide cells restricted to forested areas in the study region, that is, where forest cover within a cell exceeded 50%. The cell size was chosen to allow realistic dispersal processes at landscape scales, given estimated scales of juvenile dispersal (Table S2). Juvenile dispersal occurred among forested cells; we included forest in a 20 km buffer around the study region to reduce boundary effects. Details of modelled dispersal are provided in Appendix S1.

We used a females-only model with parameters for clutch size and nest success of first and second nesting attempts, brood survival, adult breeding season survival, juvenile dispersal and non-breeding season survival (Fig. S1), with an annual census in the spring to match the annual monitoring data. All parameters varied stochastically among grid cells and years according to defined distributions, but dynamics attributable to environmental variation arose only from the nest success and non-breeding survival GAMs. We assigned the annual, location-specific climate and housing density values to each grid cell and then used the highest-support GAM for each of these two vital rates to predict rates for each year in each grid cell. Thus, predicted vital rates varied with changing conditions. The GAM point prediction and standard error were both calculated, to define distributions from which stochastic values were drawn during simulation runs. Prediction to any environmental conditions observed in the study area, not only those represented in the original vital rate studies, allowed us to explore hypotheses relating cycling dynamics to the effect of varying climatic conditions both historically and into the future (Fig. 2).

Clutch sizes, breeding season adult survival rate and dispersal distance were drawn from fixed distributions with mean, standard deviation and range determined from reported values (Table S2), due to insufficient sample sizes for relating these parameters to environmental covariates. We also lacked data to model brood survival, but there is reason to expect that climate influences should be similar to those for nest success. Therefore, to better capture variation in fecundity, we used the dynamic nest success model to predict brood survival probabilities.

We initiated simulations in 1960 with 300,000 individuals evenly distributed throughout the study region, providing a burn-in period (1960–1981) to limit the influence of initial condition settings on model results. Model outcomes after 1970 were insensitive to plausible variations in initial distribution and abundance; the earliest model evaluation year was 1982. Simulations were run to 2012 for model

evaluation, using the PRISM data to represent climate variability. For future forecasts, we ran the same simulations to 2069, using the same GAMs for vital rate prediction, but utilizing the CMIP5 climate model output. Due to fundamental differences in the historical (PRISM) and future (CMIP5) climate models, we did not expect the evaluation period and future model results to be directly comparable in terms of estimated abundances. Rather, we expected comparability in terms of long-term patterns of variability, including changes in cycling and spatial synchrony. We used mean cell values from 500 simulations to analyse model results.

To further examine the influence of climate variability on demographic model outcomes expressed through climate sensitivities of the modelled vital rates, we ran a 'no-climate' parameterization, in which the vital rate GAMs were absent, so that there was no external forcing on vital rate variation. We also ran model variations in which the GAM-predicted vital rate values were included but randomized among years so that climate-driven vital rate variability was maintained, but with a randomized temporal structure. Details are provided in Appendix S1.

Model evaluation

Ruffed Grouse monitoring data, collected using standardized methods by the Minnesota, Wisconsin and Michigan state natural resources agencies, were available for 304 sites, spanning 1982–2012 in Minnesota, 1990–2012 in Michigan and 1994–2012 in Wisconsin (Fig. 1). Each site (a route with 10 stops) was surveyed once per year, although data were missing for some years at some sites. Monitoring data details are provided in Appendix S1.

We calculated the predicted annual abundance from the demographic model for the same landscape sampled by each monitoring site, as the mean population size (N) for the 50 model cells nearest the survey route centroid. This standardized area included the landscape sampled by the survey route without extending significantly beyond it. We gave model output a missing data structure identical to that of the monitoring data by assigning no-data values to unsurveyed site–year combinations. We summarized temporal abundance variation in both the monitoring data and model predictions using the annual mean and variance of detections (monitoring data) and N (model predictions), across the entire study area and within four latitudinal bands, choosing latitudinal bands so that sites were evenly divided ($n = 76$ sites per band; Fig. 1). We also summarized the Minnesota sites, to take advantage of the longer time series. Comparing male-only field detections with female-only model results assumes correspondence of interannual variation in male and female abundances over broad scales, consistent with studies that have found no gender differences in survival (Devers *et al.*, 2007).

In assessing population indices from the monitoring data and model output, we were interested in multiannual cycling patterns rather than minor year-to-year variation. We therefore examined trends in the smoothed data using GAMs, with a Poisson error distribution and with year as the univariate predictor (Wood, 2006). Smooth function parameterization was the same as described for the vital rate GAMs. We assessed correlation between the two smoothed data sets using the Pearson product–moment correlation of their respective model-fitted values and permutation-derived P-values with 9999 permutations. The permutation method randomized across but not within sites, retaining the temporal autocorrelation structure of the time series, for a correct type I error rate (Gouhier & Guichard, 2014).

We examined periodicities of the data series by identifying spectral peaks in their periodograms. The statistical significance of periodogram peaks was assessed by comparison against a maximum-likelihood fitted Ornstein-Uhlenbeck state space (OUSS) null model (Louca & Doebeli, 2015). The OUSS models stochastic variation accounting for temporal (between-measurements) correlation. We generated 999 permutations of the fitted null models to calculate P-values. Periodogram analyses were conducted using the PEACOTS package in R (Louca & Doebeli, 2015).

Spatial synchrony across the entire study area was assessed by examining spatial autocorrelation in the raw, site-level time series data (Bjornstad *et al.*, 1999; Gouhier & Guichard, 2014). We constructed correlograms using 40-km lag distance bins, Pearson cross-correlation among time series and permutation-based P-values (999 permutations). To examine latitudinal variation in synchrony, we calculated the cross-correlations among sites, within latitudinal bands (Fig. 1), including only the first five lag distance bins, which accounted for the strong majority of synchrony in the full data set. The site–site distance structures of the latitudinal bands differed, so we used repeated-measures ANOVA to test for the effect of latitude on synchrony, within lag distance bins, allowing for a distance-controlled comparison of overall synchrony across latitudes. Tests for association between monitoring and model time series, including spatial synchrony analyses, were conducted using the SYNCHRONY package and base functions in R (Gouhier & Guichard, 2014; R Core Team, 2014).

RESULTS

Sensitivity of vital rates to climate and land use variability

The non-breeding survival model with the strongest support included the interactive effects of winter precipitation and temperature, plus housing density (Table 1, Fig. 2). Only the two models that included the precipitation and temperature tensor product smooth term had strong support, with relative importance (summed Akaike weights) as follows: *te*(mintemp, minprecip) ($\Sigma w_i = 1.0$), housing density ($\Sigma w_i = 0.875$), *s*(mintemp) ($\Sigma w_i = 0.00$), *s*(minprecip) ($\Sigma w_i = 0.00$). As expected, non-breeding survival was lower in landscapes with higher housing density ($\beta = -0.576$,

SE = 0.198). The prediction surface for this model suggested a complex interaction between temperature and precipitation effects on non-breeding survival (Fig. 2c), generally supporting the hypothesized relationship (Fig. 2a). Higher non-breeding survival was associated with cold, snowy winter conditions as well as warm, dry conditions; lower survival was predicted for unusually cold winters with little snow, as well as unusually warm, wet winters. We used this top model for non-breeding survival prediction in the demographic model.

Nest success models that included climate variable interactions did not have strong support. The two models with strictly additive structure had strongest support, given the data, and variable importance was as follows: *s*(maxtemp) ($\Sigma w_i = 0.719$), *s*(maxprecip) ($\Sigma w_i = 0.719$), housing density ($\Sigma w_i = 0.326$), *te*(maxtemp, maxprecip) ($\Sigma w_i = 0.253$). One of the two well-supported models included housing density, but the relationship with nest success was weak ($\beta = -0.008$, SE = 0.097), so we chose to use the climate-only model for nest success prediction in the demographic model. The unimodal response of nest success to temperature variation (Fig. 2d) reflecting lower nest success during abnormally cold or hot summer seasons agreed with our expectation (Fig. 2b), whereas the *U*-shaped response to precipitation variation supported only our expectation for dry breeding seasons. The prediction of high nest success during unusually wet breeding seasons was contrary to expectation, but could have reflected a response to higher vegetation productivity.

Population dynamic consequences of climate sensitivity and exposure

Minnesota monitoring data showed marked decadal periodicity in relative abundance from 1982 to 2012, and the demographic model simulated these cycles accurately ($r = 0.66$, $P = 0.001$; Table 2 and Fig. 3a). Similar results were obtained combining all sites across all three states for 1994–2012, with strong correlation between monitoring data and model predictions overall (Fig. 3b; $r = 0.67$, $P = 0.001$). When the 1994–2012 data were summarized separately for four latitudinal bands, the monitoring data showed a pattern of higher-magnitude cycling in the north, with the strongest shift between the middle two latitudinal bands (Figs 3c–f & 4c). This pattern was reflected by the demographic model, although model prediction was uncorrelated with monitoring data at the most southerly latitude ($r = -0.55$, $P = 0.995$). In that case, there was little variability evident in the monitoring data even though decadal cycling was still detected, whereas the model produced higher-magnitude variation and overestimated period frequency (Table 2). The model better predicted low-magnitude variation in the second latitudinal band ($r = 0.35$, $P = 0.070$), and prediction improved northward (third latitudinal band: $r = 0.43$, $P = 0.034$; most northerly band: $r = 0.45$, $P = 0.026$). Better model performance in the most northerly band suggested that there was little if any bias associated with a lack of vital rate studies in higher latitudes. The coefficient of variation in model-predicted mean annual abundance showed a latitudinal pattern similar to the monitoring data, with a strong increase from the two southerly to the two northerly bands; however, the third rather than the most northerly band showed the highest-magnitude variation (Fig. 4c).

Generalized additive models fitted separately to each of the four climate variables showed limited evidence of decadal variability for temperature in the coldest month of the year, but not for the remaining variables (Figs S2 & S3). No single climate variable showed close correlation with the demographic model predictions, suggesting that cycling in model predictions was not driven directly by oscillatory patterns in one of these variables. The no-climate demographic model nonetheless verified that population fluctuations in model predictions resulted from climate-driven variability in non-breeding survival and nest success, because the no-climate model produced negligible variation in mean annual

Table 2 Periodogram analysis of Ruffed Grouse population cycle intervals based on annual counts from monitoring data and from model output.

			Model forecasts		
Latitude	Monitoring 1994–2012	Model 1994–2012	2013–2031	2032–2050	2051–2069
> 47°6′	9.5 (< 0.001)	9.5 (0.003)	9.5 (< 0.001)	6.3 (0.009)	6.3 (0.036)
45°58′ to 47°6′	9.5 (0.001)	6.3 (0.53)	9.5 (0.004)	9.5 (< 0.001)	4.8 (0.52)
44°41′ to 45°58′	9.5 (0.025)	9.5 (0.74)	9.5 (0.059)	9.5 (< 0.001)	9.5 (0.001)
< 44°41′	9.5 (< 0.001)	6.3 (0.007)	9.5 (< 0.001)	9.5 (0.008)	6.3 (< 0.001)
All latitudes	9.5 (< 0.001)	6.3 (0.15)	9.5 (< 0.001)	9.5 (< 0.001)	6.3 (0.04)
	1982–2012	1982–2012			
Minnesota	10.3 (< 0.001)	10.3 (< 0.001)			

Values are the number of years at which periodicity peaked, with the associated *P*-value in parentheses. Model forecasting results were analysed in 19-year periods for comparability to the historical monitoring and model results. Given a 19-year sampling period with annual time steps, the tested periodicities were 9.5, 6.3, 4.8, 3.8, 3.2, 2.7, and 2.4 years. Given the 31-year sampling period for Minnesota, the tested periodicities were 15.5, 10.3, 7.8, 6.2. . .2.2 years.

abundance with no cycling or trend evident for the entire region or at any latitude (Fig. S4). With GAM-predicted non-breeding survival and nest success rates introduced to the demographic model but randomly permuted across years, population fluctuations occurred at scales comparable to the unpermuted model. However, they were not correlated with the monitoring data, and they showed random variation rather than periodicity (Fig. S5). Cyclic population fluctuations correlated to the monitoring data were only produced when the climate-driven vital rate predictions were included with their true temporal structure intact.

Spatial synchrony analysis of the monitoring data indicated significant spatial structure in the degree of correlation among sites (Fig. 4a). Sites separated by 200 km or less showed stronger synchrony than the mean synchrony value, with steadily declining synchrony at further distances, although correlation values were positive across all distances. When cross-correlations for all distance bins within 200 km were summarized separately for each latitudinal band, stronger synchrony was evident in the northern half of the study region, with the transition to stronger synchrony occurring almost exclusively between the middle two latitudinal bands (Fig. 4b). Surprisingly, synchrony was not highest in the most northerly latitudinal band, but immediately to its south (repeated-measures ANOVA: $F = 37.24$, $P < 0.001$; post hoc paired t-test for difference between the two southern bands: $t = -2.73$, $P = 0.053$; middle two bands: $t = -7.17$, $P = 0.002$; two northern bands: $t = 2.00$, $P = 0.116$). The full demographic model accurately predicted the spatial synchrony structure in the monitoring data, showing a similar overall mean synchrony value, and greater-than-mean synchrony values for sites separated by 160 km or less. However, synchrony was overestimated at close distances (< 200 km) and underestimated at further distances. Despite this, the latitudinal synchrony pattern was accurately predicted by the demographic model (Fig. 4b; $F = 6.82$, $P = 0.006$; post hoc paired t-test for difference between the two southern bands: $t = -0.99$, $P = 0.376$; middle two bands: $t = -6.35$, $P = 0.003$; two northern bands: $t = 0.96$, $P = 0.390$). The no-climate demographic model, in contrast, showed little evidence of spatial synchrony, an overall mean synchrony value near zero and no differences among latitudes (Fig. S6).

Forecasting of population cycling and synchrony

Future population dynamic simulations for the entire study region showed regular, decadal cycling from 2013 to approximately 2050, followed by dampening and shortening of cycles thereafter (Table 2; Fig. 3b). Cycling became dampened after approximately 2040 at the lowest latitudes (Fig. 3c), whereas no dampening was evident at the highest latitudes (Fig. 3f). The magnitude of 2013–2050 cycle peaks showed high regularity when predictions were summarized across the study region, but showed greater variability within individual latitudinal bands. When summarized across the entire forecasting time series, latitudinal variation in the predicted cycling magnitude was similar to that of the historical model, with greatest relative abundance variation in the third latitudinal band, and a large shift between the middle two bands (Fig. 4f). Similar to the historical time period, predicted future population dynamics showed little to no direct association with any single climate anomaly variable, and GAMs fitted to each climate variable showed little evidence of decadal, cyclic variability (Figs S2 & S3). Future predicted population dynamics showed strong spatial synchrony, at spatial scales similar to that of the historical monitoring data (Fig 4d). Synchrony was highest at the third latitudinal band across the entire forecasting period, but this varied irregularly for different future 19-year time periods (Fig. 4e). No clear directional change in synchrony over time was evident across the forecasting period.

DISCUSSION

Ecologists have long suspected the importance of climate in population cycling, but few studies have investigated how future climate change might alter cycling. Our findings support a close link between climate variability and cycling in a cold-adapted bird across a large region. Cyclic dynamics in our model did not result from periodicity in any single climate or land use driver (Figs S2 & S3), but rather were a cumulative result of the influences of summer and winter temperature and precipitation on key demographic processes. The interaction between winter precipitation and temperature, which we hypothesize to be indicative of variability in snow cover quality and quantity, was an important driver of overwinter survival, and ultimately of cycling. Efforts to link high-latitude population dynamics to extrinsic forcing factors have often investigated modes of climate variability (e.g. the North Atlantic Oscillation; winter weather) by matching their periodicities to the population growth rate (Sinclair *et al.*, 1993; Forchhammer *et al.*, 1998; Post & Stenseth, 1999; Hansen *et al.*, 2013; Yan *et al.*, 2013). We suggest that our approach allows a more detailed identification of climate-demography links driving cycling, synchrony and their latitudinal variability, without excluding the possibility that the regional climate variability we studied was linked to global climate oscillations (Post & Stenseth, 1999; Stenseth *et al.*, 2002).

Our demographic model predicted fundamental aspects of observed population cycling – decadal cycle intervals, the approximate timing of cycle peaks, the scale of spatial synchrony, and the latitudinal gradient in cycle magnitude and synchrony. The model performed well in northerly regions where there was limited vital rate information, suggesting applicability there of the climate relationships described by the underlying vital rate models. Nonetheless, the model was not without error, and inaccuracies were concentrated at southerly latitudes. Targeting future demographic studies to capture a broader geographic and climatic sampling space should improve modelling efforts – for example, new nest success and non-breeding survival studies could be focused on geographic gaps (Fig. 2). Similar targeting can be

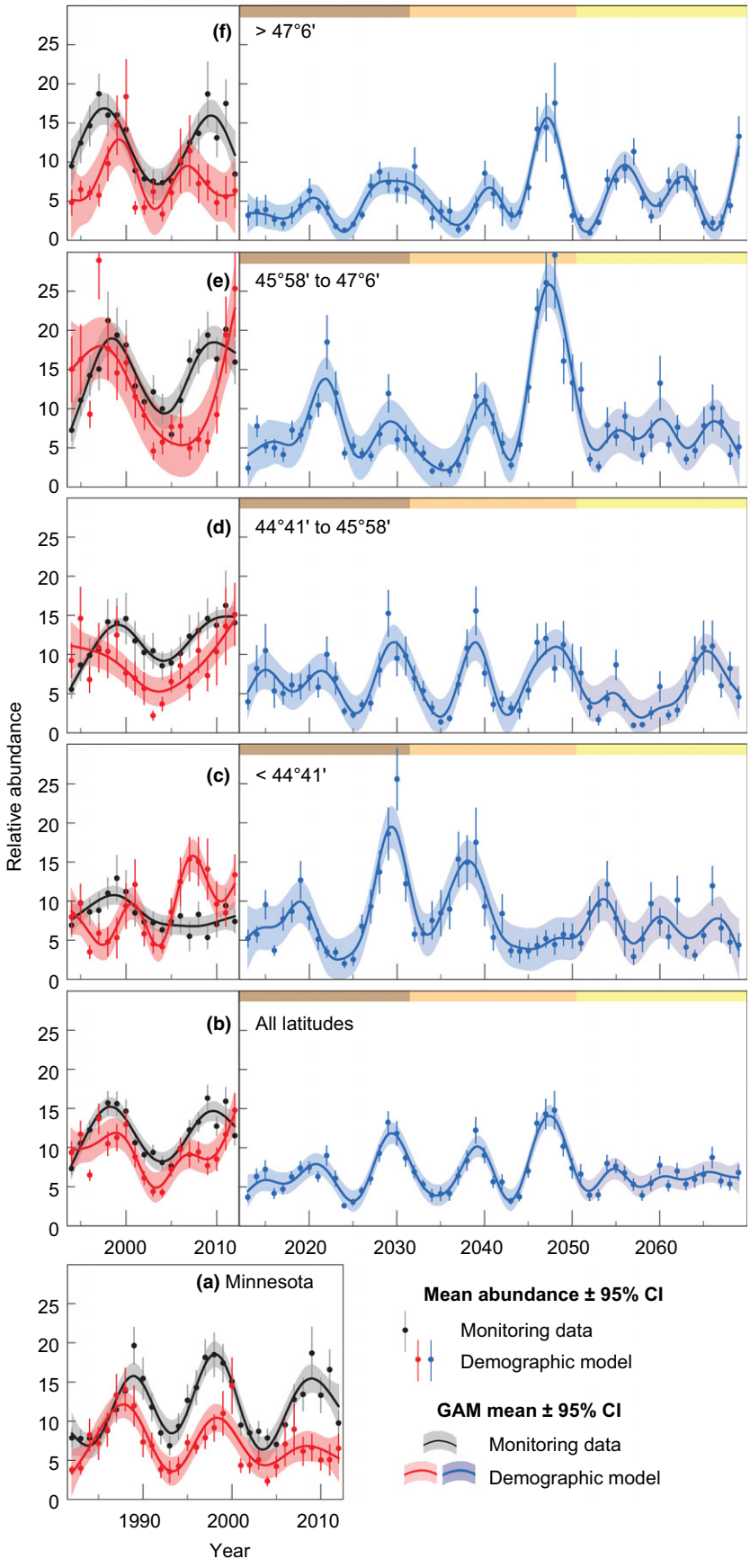

Figure 3 Ruffed Grouse demographic model predictions and monitoring data, summarized across the monitoring sites shown in Fig. 1. Cycling in the monitoring data was best predicted by the model across the longer Minnesota time series, at higher latitudes, and for all sites combined. Cycling in future model projections became desynchronized across latitudes, and dampened across all sites, after mid-century. Dots are mean (± 95% CI) relative abundance index values from the demographic model and the monitoring data. Lines are fitted values from generalized additive models (GAMs), ± 95% Bayesian confidence intervals (CI). (a) Minnesota sites, 1982–2012; (b) All sites, 1994–2012 and 2013–2069; (c–f) all sites grouped in four latitudinal bands as shown in Figure 1. Colour bars for the future projection periods correspond to the colours for the same periods in Fig. 4. The discontinuity between the 1994–2012 and 2013–2069 modelling periods results from the separate models run with PRISM and CMIP5 climate inputs, respectively, and from GAMs fitted separately to the model outputs.

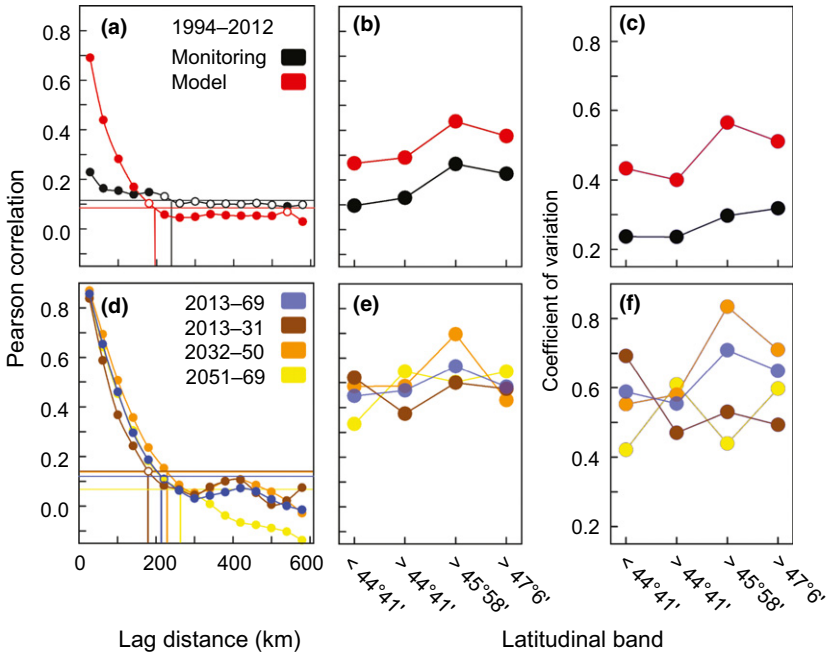

Figure 4 Spatial synchrony in Ruffed Grouse population dynamics across the study region, latitudinal variation in synchrony, and latitudinal variation in cycling magnitude for (a–c) 1994–2012 and (d–f) 2013–2069. Synchrony and cycling magnitude were generally higher at higher latitudes. The unexpected decline in synchrony between the third and the highest latitudinal bands was predicted by the climate-driven demographic model – and is likely associated with a lake effect, that is, high snowfall to the south of Lake Superior. Future prediction results are shown for three sequential 19-year periods, comparable to the historical period, and for the entire prediction period. (a, d) Spatial autocorrelation of relative abundance variation for all study sites, shown as the mean cross-correlation of time series, among sites within the indicated lag distance of one another. Solid dots are significantly ($P < 0.05$) different from the mean cross-correlation across all distances. Means across all distances are shown with horizontal lines, and vertical lines indicate the distance within which correlation is greater than the mean. (b, e) Synchrony within the four latitudinal bands shown in Fig. 1, estimated as the mean among sites within 200 km of one another, that is, the first five lag distance bands. (c, f) The coefficient of variation in relative abundance. Differences in absolute values (as opposed to patterns of variability) between the 1994–2012 and 2013–2069 modelling periods should be ignored, as they are due to basic differences in the PRISM and CMIP5 climate model inputs. Similarly, differences in absolute values between monitoring data and model output are less important than comparison of the respective patterns of variation across latitudes and among distance bands.

employed for other vital rates that cannot be modelled using existing data, or that require simplifying assumptions such as equivalency of adult and juvenile survival. Better knowledge of environmental drivers of spatio-temporal variability across the spectrum of demographic parameters should improve understanding of large-scale population dynamics.

It is notable that our model performed well without any parameterization of density dependence or time lag effects or adjustments, but with spatio-temporal variability in vital rates driven by climate. This indicates that climate variability is a crucial driver of cycling, without negating the importance of predator–prey dynamics and density dependence. Modelled cycles were more variable in magnitude and periodicity than were observed cycles, and while we suggest that climate variability induces cycling and entrains its timing, density dependence effects may further enforce cycle regularity, for example, through dampening (Yan *et al.*, 2013).

Explanations for latitudinal cycling gradients have focused on southward shifts from specialized to generalist predator communities and a corresponding strengthening of direct density dependence and/or weakening of delayed density dependence; decline in winter snow cover and length of winter; and interactions between predator communities and winter weather (Hansson & Henttonen, 1985; Williams *et al.*, 2004; Ims *et al.*, 2008). We found both cycling and synchrony gradients in Ruffed Grouse. Stronger model-predicted synchrony in particular indicates more pronounced climate influences at higher latitudes, suggesting a Moran effect (Koenig, 2002; Stenseth *et al.*, 2002). This may be consistent with a system driven partly by greater predator–prey specialization at higher latitudes if that geographic transition is mediated by the increasing prevalence of snowy winter conditions (Hansson & Henttonen, 1985). This could explain the better performance of our climate-driven model at higher latitudes if the climate-demography links we explored are stronger where snow cover is a more important determinant of dynamics. The abrupt shift in population cycling and synchrony magnitudes between the middle two latitudinal bands was unexpected, but was predicted by the climate-driven demographic model (Fig. 4). This accords with the notion

that the broader latitudinal cycling gradient is driven by winter climate differences. Many of the monitoring sites in the second-highest latitudinal band, where synchrony peaked, are south of Lake Superior in Michigan's Upper Peninsula and northern Wisconsin; this region shows a pronounced lake effect which induces high snowfall, evident in both historical data and future model projections (Notaro *et al.*, 2014).

Higher dispersal rates in the more contiguous forests at northerly latitudes (Fig. 1) could also contribute to stronger synchrony (Earn *et al.*, 2000). However, our no-climate model included the same forest cover and dispersal parameterizations as the full model, but resulted in no latitudinal differences in synchrony (Fig. S6). In addition, the spatial pattern of forest fragmentation, and thus dispersal, was fixed through time. Population synchronization, in contrast, fluctuated over time with climate variability in our future projections, and while it usually remained higher at higher latitudes, this was not always true. It is likewise possible that dispersal limitation in more fragmented habitats contributes to cycle dampening at southerly latitudes. This could result if dispersal limitation produces within-region asynchrony (Earn *et al.*, 2000), precluding cycle detection at a regional scale. Our model should have captured any such effect, since the spatial pattern of forest fragmentation constrained dispersal. We cannot therefore confidently attribute the model's prediction of dampening at lower latitudes to climate alone. However, in eastern North America, cycling declines with latitude across the Ruffed Grouse range, regardless of forest fragmentation. For example, populations do not cycle in the heavily forested southern Appalachian Mountains (Devers *et al.*, 2007).

Future projections suggest that while population cycling and synchrony will remain correlated and geographically structured, climate change is likely to alter important aspects of this system. Forecasts showed variation over time in the latitudinal synchrony gradient, and this spatio-temporal variation was positively related to the magnitude of cycling (Fig. 4e,f). We interpret these patterns in terms of climate forcing and the Moran effect: stronger climate variability should entrain both stronger variability in population size and stronger synchrony.

The future projections suggest a loss of regular decadal cycling after approximately mid-century (Fig. 3, Table 2). This resulted from processes at both of the spatial scales we examined. At the closer between-site distances within individual latitudinal bands, predicted population synchrony is high (Fig. 4d). At this scale, the variability in population size after 2050 is dampened in some latitudinal bands and remains high in others, while the clearly decadal timing of cycling evident before 2050 becomes irregular, with cycle period shortening in most cases. Comparing latitudinal bands, and thus examining larger between-site distances, population peaks are highly synchronous before 2040, then increasingly asynchronous. This is reflected in increasingly low or even negative synchrony at larger between-site distances for the entire region, particularly after 2050 (Fig. 4d). Thus, the cycle dampening apparent across the entire region is partly a result of the desynchronization of dynamics among latitudes, rather than a loss of cycling per se. Nonetheless, the regional dampening of cycles due in part to cycle shortening is consistent with observations of other species for which cycles collapse via shortening at southerly latitudes (Ims *et al.*, 2008).

Our results confirm that population cycling and synchrony are intertwined, and the loss of cycling at regional scales may co-occur with increasing regional asynchrony (Bjornstad *et al.*, 1999; Bierman *et al.*, 2006). In the case of Ruffed Grouse, this link appears to derive from the impact of climate variability – most importantly winter weather conditions – on demographic rates over space and time and is consistent with a Moran effect. The representative concentration pathway (4.5) utilized for future model projections is a moderate climate warming scenario, and our projections may therefore be considered conservative with respect to potential cycle disruptions. A winter warming trend and shifts in snow cover conditions and climate extremes have already been observed and will likely continue in the study region (Lorenz *et al.*, 2009; Tingley & Huybers, 2013; Notaro *et al.*, 2014; Fischer & Knutti, 2015). Modern climate change in this region, as in others, will affect northerly adapted species demographics, with altered patterns of population synchrony and degradation of population cycling being possible outcomes. Consequences of such changes for long-term population trends are uncertain, but recent cases of dampened cycling have been considered harbingers of future population declines, with important consequences for the trophic interactions and ecosystems in which cycling species play crucial roles (Ims *et al.*, 2008). In the Northern Hemisphere, the potential consequences of dampened cycling in response to rapidly warming winters add urgency to the need to quantify the broader impacts of climate change on cycling species.

ACKNOWLEDGEMENTS

Nathan Schumaker gave extensive advice on HexSim parameterization and modelling. Jesse Koyen assisted with data organization. The Upper Midwest and Great Lakes Landscape Conservation Cooperative provided support through a grant to the University of Wisconsin-Madison. Additional support was provided by the Wisconsin DNR through USFWS Wildlife Restoration Grant W-160-P-21. Ruffed Grouse monitoring data were made available by the WDNR, Minnesota DNR and Michigan DNR. Housing density data were provided by the Spatial Analysis for Conservation and Sustainability Lab at the University of Wisconsin-Madison. We acknowledge the World Climate Research Programme's Working Group on Coupled Modelling, which is responsible for CMIP, and the climate modelling groups for making available their model output. For CMIP, the U.S. Department of Energy's Program for Climate Model Diagnosis and Intercomparison provides coordinating support and led development of software infrastructure in partnership with the Global Organization for Earth System Science Portals.

REFERENCES

Aars, J. & Ims, R.A. (2002) Intrinsic and climatic determinants of population demography: the winter dynamics of tundra voles. *Ecology*, **83**, 3449–3456.

Bierman, S.M., Fairbairn, J.P., Petty, S.J., Elston, D.A., Tidhar, D. & Lambin, X. (2006) Changes over time in the spatiotemporal dynamics of cyclic populations of field voles (*Microtus agrestis* L.). *The American Naturalist*, **167**, 583–590.

Bjornstad, O.N., Ims, R.A. & Lambin, X. (1999) Spatial population dynamics: analyzing patterns and processes of population synchrony. *Trends in Ecology and Evolution*, **14**, 427–432.

Burnham, K.P. & Anderson, D.R. (2002) *Model selection and inference: a practical information-theoretic approach*. Springer-Verlag, New York.

Cornulier, T., Yoccoz, N.G., Bretagnolle, V., Brommer, J.E., Butet, A., Ecke, F., Elston, D.A., Framstad, E., Henttonen, H. & Hörnfeldt, B. (2013) Europe-wide dampening of population cycles in keystone herbivores. *Science*, **340**, 63–66.

Daly, C., Halbleib, M., Smith, J.I., Gibson, W.P., Doggett, M.K., Taylor, G.H., Curtis, J. & Pasteris, P.P. (2008) Physiographically sensitive mapping of climatological temperature and precipitation across the conterminous United States. *International Journal of Climatology*, **28**, 2031–2064.

Devers, P.K., Stauffer, D.F., Norman, G.W., Steffen, D.E., Whitaker, D.M., Sole, J.D., Allen, T.J., Bittner, S.L., Buehler, D.A., Edwards, J.W., Figert, D.E., Friedhoff, S.T., Giuliano, W.W., Harper, C.A., Igo, W.K., Kirkpatrick, R.L., Seamster, M.H., Spiker, H.A., Swanson, D.A. & Tefft, B.C. (2007) Ruffed grouse population ecology in the Appalachian Region. *Wildlife Monographs*, **168**, 1–36.

Dormann, C.F., Elith, J., Bacher, S., Buchmann, C., Carl, G., Carre, G., Marquez, J.R.G., Gruber, B., Lafourcade, B., Leitao, P.J., Munkemuller, T., McClean, C., Osborne, P.E., Reineking, B., Schroder, B., Skidmore, A.K., Zurell, D. & Lautenbach, S. (2013) Collinearity: a review of methods to deal with it and a simulation study evaluating their performance. *Ecography*, **36**, 27–46.

Earn, D.J., Levin, S.A. & Rohani, P. (2000) Coherence and conservation. *Science*, **290**, 1360–1364.

Fischer, E.M. & Knutti, R. (2015) Anthropogenic contribution to global occurrence of heavy-precipitation and high-temperature extremes. *Nature Climate Change*, **5**, 560–564.

Forchhammer, M.C., Stenseth, N.C., Post, E. & Langvatn, R. (1998) Population dynamics of Norwegian red deer: density-dependence and climatic variation. *Proceedings of the Royal Society B: Biological Sciences*, **265**, 341–350.

Fordham, D.A., Akçakaya, H.R., Araújo, M.B., Keith, D.A. & Brook, B.W. (2013) Tools for integrating range change, extinction risk and climate change information into conservation management. *Ecography*, **36**, 956–964.

Gouhier, T.C. & Guichard, F. (2014) Synchrony: quantifying variability in space and time. *Methods in Ecology and Evolution*, **5**, 524–533.

Hannon, S. & Martin, K. (2006) Ecology of juvenile grouse during the transition to adulthood. *Journal of Zoology*, **269**, 422–433.

Hansen, B.B., Grøtan, V., Aanes, R., Sæther, B.-E., Stien, A., Fuglei, E., Ims, R.A., Yoccoz, N.G. & Pedersen, Å.Ø. (2013) Climate events synchronize the dynamics of a resident vertebrate community in the High Arctic. *Science*, **339**, 313–315.

Hansson, L. & Henttonen, H. (1985) Gradients in density variations of small rodents: the importance of latitude and snow cover. *Oecologia*, **67**, 394–402.

Hartmann, D., Klein Tank, A., Rusticucci, M., Alexander, L., Brönnimann, S., Charabi, Y., Dentener, F., Dlugokencky, E., Easterling, D., Kaplan, A., Soden, B., Thorne, P., Wild, M. & Zhai, P. (2013) Observations: atmosphere and surface. *Climate Change 2013: The Physical Science Basis. Contribution of Working Group I to the Fifth Assessment Report of the Intergovernmental Panel on Climate Change* (ed. by T.F. Stocker, D. Qin, G.K. Plattner, M. Tignor, S.K. Allen, J. Boschung, A. Nauels, Y. Xia, V. Bex and P.M. Midegley), pp. 159–254. Cambridge University Press, Cambridge, UK and New York, NY, USA.

Ims, R.A., Henden, J.-A. & Killengreen, S.T. (2008) Collapsing population cycles. *Trends in Ecology and Evolution*, **23**, 79–86.

Jenouvrier, S. (2013) Impacts of climate change on avian populations. *Global Change Biology*, **19**, 2036–2057.

Kapnick, S.B. & Delworth, T.L. (2013) Controls of global snow under a changed climate. *Journal of Climate*, **26**, 5537–5562.

Kausrud, K.L., Mysterud, A., Steen, H., Vik, J.O., Ostbye, E., Cazelles, B., Framstad, E., Eikeset, A.M., Mysterud, I., Solhoy, T. & Stenseth, N.C. (2008) Linking climate change to lemming cycles. *Nature*, **456**, 93–97.

Keith, L.B. & Rusch, D.H. (1989) Predation's role in the cyclic fluctuations of ruffed grouse. *Proceedings of the International Ornithological Congress*, **19**, 699–732.

Koenig, W.D. (2002) Global patterns of environmental synchrony and the Moran effect. *Ecography*, **25**, 283–288.

Koenig, W.D. & Liebhold, A.M. (2016) Temporally increasing spatial synchrony of North American temperature and bird populations. *Nature Climate Change*, **6**, 614–617.

Krasting, J.P., Broccoli, A.J., Dixon, K.W. & Lanzante, J.R. (2013) Future changes in Northern Hemisphere snowfall. *Journal of Climate*, **26**, 7813–7828.

Krebs, C.J. (2011) Of lemmings and snowshoe hares: the ecology of northern Canada. *Proceedings of the Royal Society B: Biological Sciences*, **278**, 481–489.

Krebs, C.J., Boonstra, R., Boutin, S. & Sinclair, A.R.E. (2001) What drives the 10-year cycle of snowshoe hares? *BioScience*, **51**, 25–35.

Lindström, E.R. & Hörnfeldt, B. (1994) Vole cycles, snow depth and fox predation. *Oikos*, **70**, 156–160.

Lorenz, D.J., Vavrus, S.J., Vimont, D.J., Williams, J.W., Notaro, M., Young, J.A., DeWeaver, E.T. & Hopkins, E.J. (2009) Wisconsin's changing climate: temperature. *Understanding climate change: climate variability*,

predictability, and change in the midwestern United States (ed. by S.C. Pryor), pp. 76–87. Indiana University Press, Bloomington, IN.

Louca, S. & Doebeli, M. (2015) Detecting cyclicity in ecological time series. *Ecology*, **96**, 1724–1732.

Ludwig, G.X., Alatalo, R.V., Helle, P., Lindén, H., Lindström, J. & Siitari, H. (2006) Short- and long-term population dynamical consequences of asymmetric climate change in black grouse. *Proceedings of the Royal Society B: Biological Sciences*, **273**, 2009–2016.

Lurgi, M., Brook, B.W., Saltré, F. & Fordham, D.A. (2015) Modelling range dynamics under global change: which framework and why? *Methods in Ecology and Evolution*, **6**, 247–256.

McRae, B.H., Schumaker, N.H., McKane, R.B., Busing, R.T., Solomon, A.M. & Burdick, C.A. (2008) A multi-model framework for simulating wildlife population response to land-use and climate change. *Ecological Modelling*, **219**, 77–91.

Notaro, M., Lorenz, D., Hoving, C. & Schummer, M. (2014) Twenty-first-century projections of snowfall and winter severity across central-eastern North America. *Journal of Climate*, **27**, 6526–6550.

Post, E. & Forchhammer, M.C. (2004) Spatial synchrony of local populations has increased in association with the recent Northern Hemisphere climate trend. *Proceedings of the National Academy of Sciences USA*, **101**, 9286–9290.

Post, E. & Stenseth, N.C. (1999) Climatic variability, plant phenology, and northern ungulates. *Ecology*, **80**, 1322–1339.

Post, E., Forchhammer, M.C., Bret-Harte, M.S. *et al.* (2009) Ecological dynamics across the Arctic associated with recent climate change. *Science*, **325**, 1355–1358.

Pryor, S.C., Kunkel, K.E. & Schoof, J.T. (2009) Did precipitation regimes change during the twentieth century? *Understanding climate change: climate variability, predictability, and change in the midwestern United States* (ed.by S.C. Pryor), pp. 100–112. Indiana University Press, Bloomington, IN.

Pulliam, H.R., Dunning, J.B., Jr & Liu, J. (1992) Population dynamics in complex landscapes: a case study. *Ecological Applications*, **2**, 165–177.

R Core Team (2014) *R: a language and environment for statistical computing*. R Foundation for Statistical Computing, Vienna, Austria. http://www.R-project.org. (accessed 1 June 2015).

Radeloff, V.C., Stewart, S.I., Hawbaker, T.J., Gimmi, U., Pidgeon, A.M., Flather, C.H., Hammer, R.B. & Helmers, D.P. (2010) Housing growth in and near United States protected areas limits their conservation value. *Proceedings of the National Academy of Sciences USA*, **107**, 940–945.

Ranta, E., Kaitala, V., Lindstrom, J. & Linden, H. (1995) Synchrony in population dynamics. *Proceedings of the Royal Society B: Biological Sciences*, **262**, 113–118.

Rusch, D.H., Destefano, S., Reynolds, M.C. & Lauten, D. (2000) Ruffed Grouse (*Bonasa umbellus*). *The birds of North America online* (ed. by A. Poole). Cornell Lab of Ornithology, Ithaca; retrieved from the Birds of North America Online: http://bna.birds.cornell.edu/bna/species/515. doi:10.2173/bna.515. (accessed 1 December 2013).

Schurr, F.M., Pagel, J., Cabral, J.S., Groeneveld, J., Bykova, O., O'Hara, R.B., Hartig, F., Kissling, W.D., Linder, H.P., Midgley, G.F., Schroder, B., Singer, A. & Zimmermann, N.E. (2012) How to understand species' niches and range dynamics: a demographic research agenda for biogeography. *Journal of Biogeography*, **39**, 2146–2162.

Selwood, K.E., McGeoch, M.A. & Mac Nally, R. (2014) The effects of climate change and land-use change on demographic rates and population viability. *Biological Reviews*, **90**, 837–853.

Sinclair, A.R.E., Gosline, J.M., Holdsworth, G., Krebs, C.J., Boutin, S., Smith, J.N.M., Boonstra, R. & Dale, M. (1993) Can the solar cycle and climate synchronize the Snowshoe Hare cycle in Canada? Evidence from tree rings and ice cores. *The American Naturalist*, **141**, 173–198.

Stenseth, N.C., Mysterud, A., Ottersen, G., Hurrell, J.W., Chan, K.-S. & Lima, M. (2002) Ecological effects of climate fluctuations. *Science*, **297**, 1292–1296.

Taylor, K.E., Stouffer, R.J. & Meehl, G.A. (2012) An overview of CMIP5 and the experiment design. *Bulletin of the American Meteorological Society*, **93**, 485–498.

Thomas, V.G. (1987) Similar winter energy strategies of grouse, hares and rabbits in northern biomes. *Oikos*, **50**, 206–212.

Thompson, F.R. & Fritzell, E.K. (1988) Ruffed grouse winter roost site preference and influence on energy demands. *Journal of Wildlife Management*, **52**, 454–460.

Tingley, M.P. & Huybers, P. (2013) Recent temperature extremes at high northern latitudes unprecedented in the past 600 years. *Nature*, **496**, 201–205.

Tirpak, J.M., Giuliano, W.M., Miller, C.A., Allen, T.J., Bittner, S., Buehler, D.A., Edwards, J.W., Harper, C.A., Igo, W.K., Normar, G.W., Seamster, M. & Stauffer, D.F. (2006) Ruffed grouse population dynamics in the central and southern Appalachians. *Biological Conservation*, **133**, 364–378.

Tyler, N.J.C., Forchhammer, M.C. & Øritsland, N.A. (2008) Nonlinear effects of climate and density in the dynamics of a fluctuating population of Reindeer. *Ecology*, **89**, 1675–1686.

Viterbi, R., Imperio, S., Alpe, D., Bosser-peverelli, V. & Provenzale, A. (2015) Climatic control and population dynamics of black grouse (*Tetrao tetrix*) in the Western Italian Alps. *The Journal of Wildlife Management*, **79**, 156–166.

Williams, C.K., Ives, A.R., Applegate, R.D. & Ripa, J. (2004) The collapse of cycles in the dynamics of North American grouse populations. *Ecology Letters*, **7**, 1135–1142.

Williams, S.E., Shoo, L.P., Isaac, J.L., Hoffmann, A.A. & Langham, G. (2008) Towards an integrated framework for assessing the vulnerability of species to climate change. *PLoS Biology*, **6**, 2621–2626.

Wood, S.N. (2006) *Generalized additive models: an introduction with R*. CRC Press, Boca Raton, FL.

Yan, C., Stenseth, N.C., Krebs, C.J. & Zhang, Z. (2013) Linking climate change to population cycles of hares and lynx. *Global Change Biology*, **19**, 3263–3271.

Zimmerman, G.S., Horton, R.R., Dessecker, D.R. & Gutierrez, R.J. (2008) New insight to old hypotheses: ruffed grouse population cycles. *The Wilson Journal of Ornithology*, **120**, 239–247.

Zuur, A.F., Ieno, E.N., Walker, N.J., Saveliev, A.A. & Smith, G.M. (2009) *Mixed effects models and extensions in ecology with R*. Springer, New York, NY.

SUPPORTING INFORMATION

Additional Supporting Information may be found in the online version of this article:

Appendix S1 Methods details.

Table S1 Detailed information for studies from which nonbreeding survival and nest success rate estimates were derived.

Table S2 Estimation of vital rate parameters that were included in the demographic model, but not modelled with environmental covariates.

Figure S1 Ruffed Grouse life cycle diagram showing probabilistic vital rates parameterized in the spatially explicit demographic model.

Figure S2 Temperature and precipitation anomalies summarized across Ruffed Grouse monitoring sites shown in Fig. 1; nonbreeding survival covariates.

Figure S3 Temperature and precipitation anomalies summarized across Ruffed Grouse monitoring sites shown in Fig. 1; nest success covariates.

Figure S4 Ruffed Grouse population cycling predictions with and without climate effects, i.e., comparing the full model and the no-climate model.

Figure S5 Ruffed Grouse population cycling predictions with climate-driven vital rate predictions randomly permuted across years.

Figure S6 Ruffed Grouse spatial synchrony predictions with and without climate effects, i.e., comparing the full model and the no-climate model.

BIOSKETCHES

Lars Y. Pomara is an Ecologist at the Southern Research Station, US Forest Service. He is an ornithologist, wildlife ecologist and geographer with interests in conservation, landscape ecology, and biogeography.

Benjamin Zuckerberg is an assistant professor in the Department of Forest and Wildlife Ecology at the University of Wisconsin-Madison. His research focuses on how modern climate change and habitat loss influence wildlife behaviour, abundance, and distribution.

Editor: Diederik Strubbe